RSC Advances

PAPER

View Article Online
View Journal | View Issue

Cite this: *RSC Adv.*, 2024, **14**, 25329

Utilizing a graphene quantum dot/hydrogel nanocomposite for determination of cisplatin in urine samples

Seyed Mohammad Hossein Pourmand,[a] Nastaran Hashemzadeh,[a] Jafar Soleymani,[a] Abolghasem Jouyban,[a] Yosra Vaez-Gharamaleki[b] and Elaheh Rahimpour *[ac]

Received 12th June 2024
Accepted 5th August 2024

DOI: 10.1039/d4ra04294h

rsc.li/rsc-advances

Currently, the growth and development of cancer are rising in the world, and as a result, the use of anticancer drugs such as cisplatin has also increased. Considering that the therapeutic index of anticancer drugs is low, it is essential to design and develop an accurate and correct method to analyze and determine the concentration of anticancer drugs in the biological samples. In this study, graphene quantum dots/hydrogel nanocomposite was used to determine cisplatin concentration in urine samples. A three-dimensional network of polyvinyl alcohol hydrogel was composited with graphene quantum dots and used as a probe for the determination of cisplatin. The morphology and characterization of the probe were studied using high-resolution transmission electron microscopy, dynamic light scattering, energy-dispersive X-ray spectroscopy, and Fourier transform infrared spectroscopy. This platform showed a linear calibration curve in the range from 4.3 to 25.0 ng mL^{-1} with a detection limit of 1.2 ng mL^{-1}. The relative intra- and inter-day standard deviations of the probe for the determination of cisplatin were 1.8% and 3.6% ($n = 5$), respectively. The validated method was used for determination of cisplatin in urine samples of patients receiving this medication with acceptable results and good recoveries.

1 Introduction

Cisplatin is a heavy metal complex containing a central atom of platinum, surrounded by two chlorine and two ammonia groups in the *cis* position.[1] Cisplatin has biochemical properties similar to those of bifunctional alkylating agents producing inter-strand and intra-strand cross-links in DNA.[2] It appears to exert its cytotoxic effects by directly binding with DNA. Inhibition of DNA synthesis by cisplatin is probably accomplished by alteration in the DNA template.[3] Cisplatin has a narrow therapeutic index, which means that patients may experience toxicities even when administered at standard doses. These toxicities can affect various systems, including hearing (ototoxicity), renal, gastrointestinal, neurological, or hematological systems.[4] Determining the concentration of cisplatin in biological samples is crucial for optimal treatment outcomes. It helps monitor the drug's effectiveness and adjust dosages accordingly. Accurate measurement ensures patients receive the right amount of medication to achieve the desired therapeutic effect. Monitoring cisplatin concentration also helps identify patients at risk of developing side effects and toxicity. Research relies on precise measurements to study pharmacokinetics, pharmacodynamics, and efficacy. In clinical trials, accurate concentration measurement is critical to evaluate new treatments and patient safety. Overall, measuring cisplatin concentration is essential for ensuring patient safety, optimizing treatment, and advancing research in cancer therapy.[5] Therefore, it demands suitable techniques for the precise determination of cisplatin in various biological samples. This is essential not only to prevent their induced intoxication but also to monitor the doses. Accordingly, many different analytical techniques have been adapted for cisplatin monitoring in biological and environmental samples such as electrochemical,[6,7] liquid chromatography-mass spectrometry (LC-MS),[8] high-performance liquid chromatography (HPLC),[9,10] capillary electrophoresis,[11] spectroscopy[12] and atomic absorption spectrometry[13] procedures. Fluorescent methods with the advantages of easy operation, and the expansion of a reliable platform as a recognition element is considered in biomedical applications.[14]

With recent advances in nanotechnology, nanostructures with their superior physicochemical features to improve the selectivity and sensitivity have gained attention in constructing efficient analytical sensors. Several fluorescent nanomaterials, such as metal nanoparticles, graphene quantum dots (GQDs),

[a]*Pharmaceutical Analysis Research Center and Faculty of Pharmacy, Tabriz University of Medical Sciences, Tabriz, Iran. E-mail: rahimpour_e@yahoo.com*
[b]*Hematology–Oncology Research Center, Tabriz University of Medical Sciences, Tabriz, Iran*
[c]*Infectious and Tropical Diseases Research Center, Tabriz University of Medical Sciences, Tabriz, Iran*

and carbon quantum dots have been expansively exploited in sensor design.[15] GQDs are nanometer-sized pieces of graphene that exhibit unique properties that make them interesting candidates for a wide range of applications especially sensing processes.[16] Particles in nano dimensions have two characteristics increasing the ratio of surface to volume and dissociation of energy levels. By increasing the ratio of surface area to volume, the ratio of surface atoms in a particle increases and that particle becomes much more reactive and tends to clump[17] which can be used as an efficient platform in the sensing applications.[18,19] Hydrogels as three-dimensional (3D) polymeric matrices can afford a robust solid sensing platform while avoiding nanomaterial aggregation and holding or enhancing their fluorescent properties.[20,21] Recently, some innovative functional platforms have been introduced by combining fluorescent probes and hydrogels in which, the hydrogel matrix not only stabilized and increased the fluorescence signal of nanomaterials; but also enhanced the sensitivity and selectivity of the system.[22] In these materials, polymer is used as a matrix and nanoparticle is used as a reinforcing phase. In other words, hydrogel nanocomposite is a hydrophilic polymer network, which becomes a network physically or covalently with nanoparticles.[23]

This research aimed to develop a sensing probe for detecting cisplatin in urine samples using a novel nanocomposite hydrogel. The nanocomposite, composed of polyvinyl alcohol (PVA) hydrogel and GQDs which PVA served as the polymeric matrix, while GQD acted as a nanofiller and reinforcement with fluorescent property. Cisplatin, a widely used medication with narrow therapeutic index, was chosen as the target analyte. The validated probe was tested for its ability to detect cisplatin in urine samples from patients receiving this medication.

2 Materials and methods

2.1. Reagents and solutions

All the analytical reagent-grade chemicals were commercially achieved and used without further purification. PVA with molecular weight (M_w) of 89 000–98 000, extra pure disodium tetraborate decahydrate and citric acid (>99.5%) was provided by Merck (Darmstadt, Germany) for the synthesis of nanocomposite. A stock solution of cisplatin (1 mg mL^{-1}) was provided by Mylan Pharmaceuticals ULC which was appropriately diluted as necessary. For buffer preparation, sodium dihydrogen phosphate (Merck, Darmstadt, Germany) was used and adjusted to different pHs by sodium hydroxide (NaOH) and hydrochloric acid (HCl) which were all received from Merck (Darmstadt, Germany). Ultrapure deionized water was achieved from (Shahid Ghazi Pharmaceutical Co., Tabriz, Iran).

2.2. Apparatus and characterization

A FP-750 spectrofluorometer (Jasco Corp., Japan) was used for the measurement of the fluorescence spectra equipped with a xenon lamp source. The bandwidths were set at 10 nm in the excitation and 20 nm in emission paths for recording all fluorescence spectra using a 1 mL standard quartz cell. For pH adjustment, a model 744 digital pH meter (Metrohm Ltd, Switzerland) was used. Dynamic light scattering (DLS) and a G2F20 high resolution transmission electron microscopy (HRTEM) (Tecnai, The North American) were employed for estimating the distribution of particle size in the prepared nanocomposite and evaluating their shape and size, respectively. Powder X-ray diffraction (XRD) patterns were achieved using a Siemens diffractometer with filtered Cu-Kα radiation at 35 kV within the 2θ range of 470°. To verify the surface's functionalized groups, Fourier transforms infrared (FT-IR) spectroscopy was accomplished on Bruker Tensor 270 (KBr wafer technique) over 4000–400 cm^{-1} as spectral width.

2.3. Synthesis of GQDs

GQDs were synthesized by pyrolyzing citric acid according to a reference[24] with some modifications. Briefly, 2.0 g of citric acid was put into a beaker and heated to 230 °C by a heating mantle until the citric acid changed to an orange liquid. Then, for preparing GQDs, 30 mL of 10 mg per mL NaOH solution was added into the orange liquid dropwise with continuous, vigorous stirring. The obtained GQD solution was stable for at least one month in the refrigerator at 4 °C.

2.4. Synthesis of GQDs/PVA hydrogel nanocomposite

For this purpose, 1.2 g of PVA was weighed and then poured into a 50 mL beaker. 20 mL of distilled water was added to it and then heated on a heater at a temperature of 30 °C for 10 minutes and stirred, and after 10 minutes, it was stirred for 3 hours until a uniform and clear solution was observed at room temperature. Then 250 μL of 0.25 g mL^{-1} borax was added to the above solution. After preparing the hydrogel, 30 mL graphene quantum dot was added and stirred for 10 minutes to prepare the GQDs/PVA hydrogel nanocomposite.[25,26] The obtained hydrogel was kept at 4 °C for further experiments.

2.5. Samples preparation

To optimize and validate the proposed nanocomposite, human urine samples were provided from healthy volunteers. To investigate the applicability of the validated method, real samples were supplied from patients receiving cisplatin which asked them to collect a 24 hour urine sample. Sample donors signed a consent form approved by the Ethics Committee of the Tabriz University of Medical Sciences (IR.TBZMED.PHARMACY.REC.1402.067). Before analysis, urine samples were centrifuged and then 0.5 mL of the supernatant solution was reached 5 mL for the next step.

2.6. General procedure

The procedure was performed in a 2 mL vial as a batch method. In an optimized condition, 50 μL of 0.1 mol per L phosphate buffer (pH 7.0) was added to the microtube including 100 μL of the urine samples. Then, the 350 μL GQDs/PVA hydrogel nanocomposite was added into the above solution and the final volume was fixed to 0.6 mL with deionized water. After incubation of the sample for 5 min, the fluorescence intensity as an

analytical signal was measured at around $\lambda_{max} = 410$ nm after excitation at 320 nm. In this system, $\Delta F(F - F_0)$ was regarded as an analytical response where, F and F_0 were the probe response in the presence and absence of cisplatin, respectively. The experiments were implemented three times at room temperature and the mean of data were reported herein.

3 Results and discussions

3.1. Structural characterization of GQDs/PVA hydrogel nanocomposite

The morphology and particle size of GQDs were characterized by HRTEM measurements. Fig. 1A indicated that GQDs have mostly spherical morphology with a size of approximately less than 20 nm. It was also confirmed that the nanoscale particles were highly dispersed with no noticeable aggregation of GQDs during the synthesis process. This was further approved by size distribution in Fig. 1B in which the sizes of NPs were about <20 nm.

To confirm the crystalline structure of the nanocomposite and verify the successful incorporation of GQDs into the PVA hydrogel matrix, XRD analysis was performed on the prepared samples. The XRD pattern of the nanocomposite hydrogel showed distinct peaks at 2θ angle of 24°, which correspond to the (002) lattice planes of the GQDs.[27] Additionally, the pattern revealed peaks at 2θ angle of 19.8° which were characteristic of the orthorhombic lattice structure of PVA hydrogel.[28] Fig. 1C showed the XRD pattern for pure PVA hydrogel, GQDs and GQDs/PVA hydrogel nanocomposite approving the successful synthesis of nanocomposite.

To provide additional proof of the successful synthesis of the nanocomposite, FT-IR spectroscopy was conducted and the resulting spectra were shown in Fig. 1D. The FT-IR spectra of pure PVA hydrogel, GQDs and the prepared nanocomposites were given in this figure. The FT-IR spectrum of pure PVA hydrogel and GQDs exhibited a peak around 3450 cm^{-1}, which was attributed to the stretching vibration of the hydroxyl groups (O–H). In the nanocomposite, the intensity and broadness of this peak increased, indicating a strong interaction between the PVA hydrogel and GQDs. The broadening of the peak was likely due to the dispersion of hydrogen bond donor groups, such as –OH and –COOH, on the GQDs surfaces. This suggests that hydrogen bonding occurs between the PVA hydrogel and GQDs, which changes the position and shape of the IR absorption band. Furthermore, the FT-IR spectra showed shifts in the C–H stretching and bending peaks of pure PVA hydrogel. The C–H stretching peak shifted from 2915.58 cm^{-1} to 2850.68 cm^{-1}. Additionally, the C–O bending and stretching peaks of the acetyl group on the polymer backbone shifted from 1095.62 cm^{-1} to 1093.07 cm^{-1}. The vibration peaks between 500 cm^{-1} and 800 cm^{-1} can be attributed to either C–H rocking mode or C–C stretching which shown in both pure materials and nanocomposite structure. The FT-IR spectrum of GQD showed bands at 1640.16 cm^{-1} and 1575.68 cm^{-1}, which related to surface C=O and –COOH groups, and also appeared with a slightly shift in the nanocomposite spectrum. The peaks around 1400 cm^{-1} and 1300 cm^{-1} were assigned to –OH bending (in-

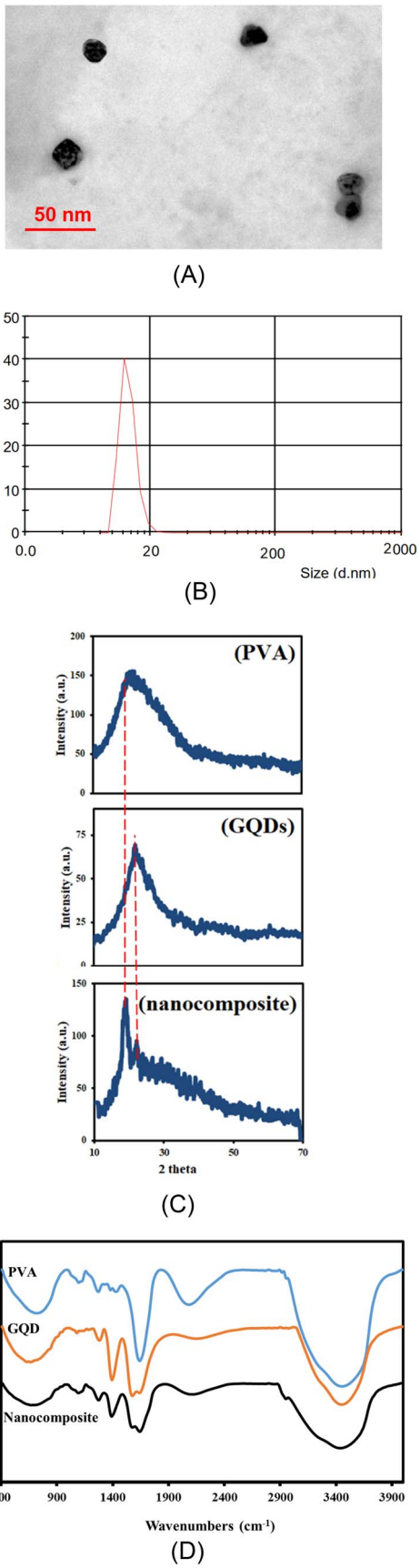

Fig. 1 Characterization analyses (A) HR-TEM image, and (B) DLS of GQDs/PVA hydrogel nanocomposite, (C) XRD pattern and (D) FT-IR spectra of PVA hydrogel, GQD and GQDs/PVA hydrogel nanocomposite.

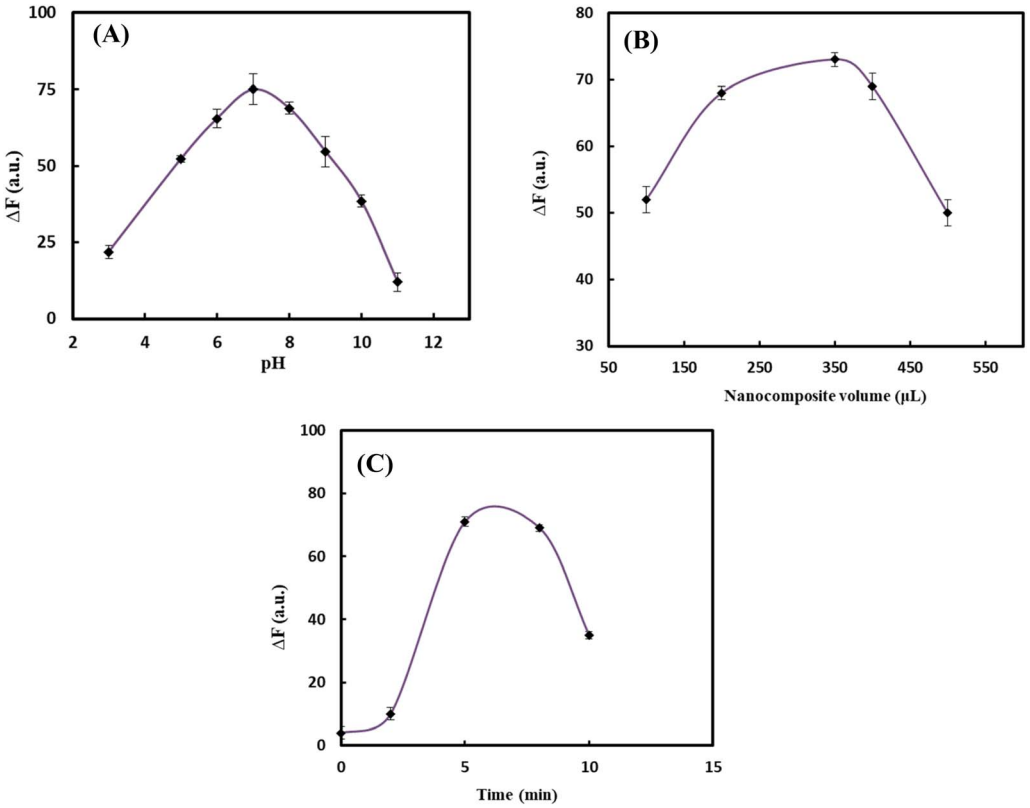

Fig. 2 Effect of (A) pH, (B) volume of nanocomposite, and (C) incubation time on the response of the probe.

plane) and C–H wagging modes that also remain identical in shape and position for both pure materials and nanocomposite. This finding was in accordance with the previous reports.[29]

3.2. Sensing mechanism

The nanocomposite used here was composed of PVA hydrogel and GQDs which PVA served as the polymeric matrix, while GQDs acted as a fluorescent nanofiller. The combination of these two components leaded to a 2.0-fold enhanced fluorescence response toward cisplatin. PVA was a polymer with excellent solubility and dispersibility in water, which allowed it to effectively prevent the GQDs from aggregating or sticking together. PVA also as a substrate providing a high availability sites for analytes to react with GQDs. This enabled enhanced reaction efficiency, improved sensitivity, and better performance in sensing applications.

When GQDs are excited, an electron is lifted from the valence band to the conduction band, leaving behind a hole. This process is followed by two distinct pathways: (i) the electron and hole can recombine in the valence band, forming excitons. These excitons can then undergo radiative decay, resulting in the emission of light, or non-radiative decay, which leads to the release of heat. (ii) Alternatively, the excited electron can become trapped by surface defects on the GQDs. This trapped electron can then undergo back transfer, which enables the reformation of excitons. These excitons can also undergo radiative decay or non-radiative decay, ultimately leading to the emission or heat release of energy.[30] Fluorescence enhancement occurs when the fluorescence intensity of a fluorophore is boosted by its interaction with another molecule. This phenomenon can arise when the surface defects of a fluorophore are passivated by the presence of an analyte. This is particularly relevant in GQDs, which often exhibit low luminescence due to the presence of surface defects. By neutralizing these defects, the fluorescence intensity of the GQDs can be significantly enhanced.[31] Some of previous works with similar mechanism were determination of Zn^{2+} ions using L-cysteine capped CdS QDs,[32] Cd^{2+} ions using three AgInZnS NPs (of different metal ratios),[33] Co^{2+}, Cd^{2+} and Pb^{2+} metal ions using MoS_2 quantum dots,[34] carbamazepine using copper nanoclusters,[35] and adenine using histidine-stabilized CdS.[36] Herein, GQDs/PVA hydrogel nanocomposite showed a distinct fluorescence band centered at 410 nm which an enhancing process was observed in its fluorescence intensity after cisplatin adding. According to the above evidence, we hypothesized that the interaction between GQDs/PVA hydrogel nanocomposite and cisplatin would lead to the blocking of non-radiative electron–hole recombination sites on the GQDs surface, ultimately resulting in an enhancement of the fluorescence intensity which was proportional to cisplatin concentration. The interaction between GQDs and cisplatin is primarily due to the coordination complexation of the platinum ion of cisplatin with functional groups present on the GQD surface (carboxyl and hydroxyl groups). Furthermore, it was reported in the literature[37] that the labile chloride ligands of cisplatin can be

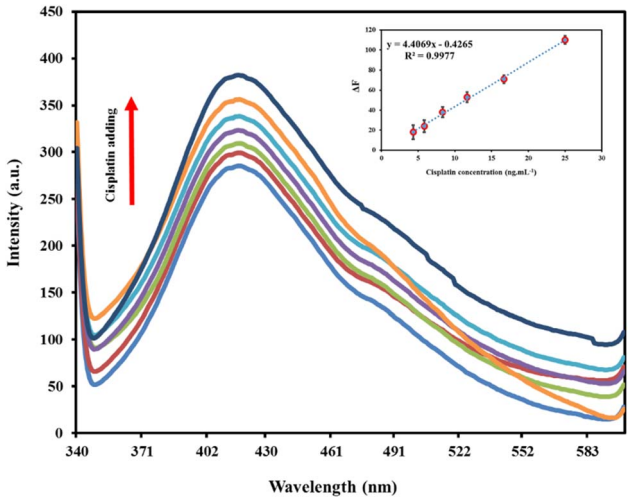

Fig. 3 Fluorescence intensity of GQDs/PVA hydrogel nanocomposite in the absence and presence of cisplatin in the range of 4.3 to 25.0 ng mL^{-1}. Inset: Calibration curve obtained for cisplatin in urine.

replaced by carboxylic groups of GQDs, forming a cisplatin/GQDs complex and resulting in the coordination of the platinum ion with the GQD surface.

3.3. Optimization of reaction conditions

To design an effective probe, it was essential to optimize the experimental conditions, as these factors have a direct impact on the probe's performance. In the initial experiments, it was discovered that the fluorescent intensity was influenced by three key factors: pH, concentration of nanocomposite, and incubation time. To optimize the conditions, a cisplatin concentration of 16.0 ng mL^{-1} as the starting point for further optimization. The effect of pH changes on the response of the probe was investigated by adjusting pH in the range of 3.0–11.0 using phosphate buffer (PBS, 0.10 mol L^{-1}). The response of the florescent probe was increased along with increasing pH in which the highest fluorescence response (ΔF) was obtained at pH 7.0 as illustrated in Fig. 2A due to the high affinity of cisplatin toward GQDs at neutral conditions.[38] As a result, pH 7.0 was selected as the optimum value and other affective variables were optimized in this pH value. To identify the optimal amount of GQDs/PVA hydrogel nanocomposite, various volumes in the range of 100–500 μL were evaluated during the design process. The results showed that the highest fluorescence response was achieved when using 350 μL of the nanocomposite, which was subsequently selected as the optimal volume (Fig. 2B). Beyond this point, fluorescence intensity decreased, likely due to probe self-quenching at high concentrations. The incubation time, which was the time required for cisplatin molecules and GQDs/PVA hydrogel nanocomposite to interact, was also optimized. By adding nanocomposite to a solution containing cisplatin and PBS at pH 7.0 for varying periods, we observed an increasing response pattern with increasing incubation time (Fig. 2C) up to 8 min. To maximize and stabilize fluorescence intensity, we recorded the signal 5 min after solution preparation. The optimized reaction conditions were found to be: pH 7.0, nanocomposite value of 350 μL, and incubation time of 5 min.

3.4. Analytical figures of merit

To assess the analytical performance of the probe towards cisplatin, the concentration-dependent behavior of the method under optimal conditions was investigated in urine matrix. As shown in Fig. 3, the fluorescence intensity of the nanocomposite at 410 nm increased linearly with the concentration of cisplatin, ranging from 4.3 to 25.0 ng mL^{-1}. A linear relationship was established between the intensity ratio and cisplatin concentration, with a regression equation of $\Delta F = 4.4069C_{\text{cisplatin}} - 0.4265 (R^2 = 0.9977)$ as can be seen in the inset picture of Fig. 3. The calculated limit of detection (LOD) and limit of quantification (LOQ) were 1.2 and 4.3 ng mL^{-1}, respectively. The precision of the method was evaluated by repeating the cisplatin determination on different days, with intra-day and inter-day relative standard deviations (RSDs%) of 1.8% and 3.6%, respectively. The results demonstrate that the proposed nanocomposite was suitable for the determination of cisplatin in urine samples. The advantages of this method include its ability to overcome limitations associated with small-sized nanoparticles, such as poor storage stability, particle–particle aggregation, and low dispersibility in solutions due to the PVA matrix as a stabilizing scaffold. Furthermore, the analytical characterization of the validated method was comparable to other reported literature-based methods, as summarized in Table 1.

Table 1 Comparison of analytical characteristics validated method with other reported techniques in the literature

Method	Sample	LOD (μg mL^{-1})	Linear range (μg mL^{-1})	Reference
HPLC-UV	Plasma	1	1–10	10
HPLC-PDA[a]	Aqueous solutions	14.0	150–451	39
Voltammetry	Serum	1.3	1.8–54.2	40
Voltammetry	Serum	0.034	0.39–7.82	6
Spectrophotometry	Biological samples	4.2	10.0–5750.0	41
Spectrofluorometry	Plasma	0.007	0.025–0.16	42
Spectrofluorometry based on GQDs/PVA hydrogel nanocomposite	Urine	0.0012	0.0043–0.025	This work

[a] High performance liquid chromatography, photodiode array detector.

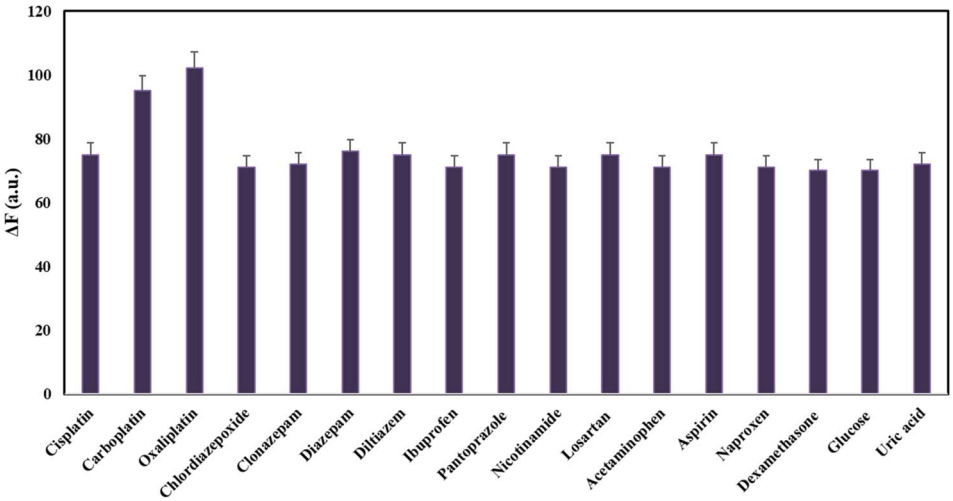

Fig. 4 Study of the method selectivity under optimal conditions in the presence of some possible interfering co-administrated drugs with concentrations of 16.0 ng mL^{-1}.

Table 2 Effect of the potential and available interfering existing alone on the fluorescence intensity of GQDs/PVA hydrogel nanocomposite (ΔF values)

Interfering drugs	ΔF
Carboplatin	+19
Oxaliplatin	+32
Chlordiazepoxide	−4.0
Clonazepam	−4.9
Diazepam	+3.0
Diltiazem	−3.2
Ibuprofen	−3.8
Pantoprazole	+2.9
Nicotinamide	−4.1
Losartan	−3.4
Acetaminophen	−3.1
Aspirin	+4.4
Naproxen	−5.7
Dexamethasone	−6.5
Glucose	−5.1
Uric acid	−4.9

3.5. Interference study with coexisting substances

To investigate the specificity and selectivity of the established fluorescent method, it was required to study the interfering effect of possible co-administrated drugs with cisplatin in the same condition. To evaluate the selectivity, the responses toward the potential and available interfering substances including carboplatin, oxaliplatin, chlordiazepoxide, clonazepam, diazepam, diltiazem, ibuprofen, pantoprazole, nicotinamide, losartan, acetaminophen, aspirin, naproxen, and dexamethasone was recorded and interpreted. The responses of the proposed probe were assessed in a drug concentration of 16.0 ng mL^{-1}. As shown in Fig. 4, the addition of most interferes has a negligible effect on the fluorescence response of the nanoprobe. However, in the case of simultaneous administration of carboplatin and oxaliplatin with cisplatin, it causes interference in analyte evaluation. It means that the method was unable to distinguish between these three drugs and may not be able to accurately quantify the amount of present cisplatin. To overcome this limitation, one can use different separation and/or extraction techniques to accurately detect and quantify these three drugs. In general, the results revealed relatively good selectivity toward cisplatin determination in the presences of some other possible co-administrated drugs. In order to explore more on the selectivity of the established fluorescent method, the ΔF values, when the potential and available interfering was existing alone, was determined and reported in Table 2. As can be seen, the ΔF values for most interferes (except for carboplatin and oxaliplatin) were non-significant amounts confirming the method selectivity for cisplatin determination.

3.6. Analytical application

The validate method was successfully used to analyze urine samples with known concentrations of cisplatin. To assess the accuracy of the method, recovery tests were conducted by adding specific amounts of cisplatin to the samples. The results are

Table 3 Determination of cisplatin in spiked urine samples

Sample	Added (ng mL^{-1})	Found ± SD (ng mL^{-1})	Recovery[a] (%)	t-Test[b]
Urine 1				
	6.0	6.2 ± 0.10	103.0	3.46
	12.0	12.7 ± 0.62	105.8	1.95
Urine 2				
	6.0	6.3 ± 0.21	105.0	2.47
	12.0	12.2 ± 0.25	101.6	1.38

[a] Mean of three determinations ± standard deviation. [b] t-Critical = 4.3 for $n = 3$ and $P = 0.05$.

Table 4 Determination of cisplatin in real urine samples by validated method

No.	Gender	Co-administrated drugs	Found ($\mu g\ mL^{-1}$)
1	Male	Gemcitabine	3.1 ± 0.08
2	Female	Paclitaxel	1.8 ± 0.1
3	Female	Paclitaxel	2.0 ± 0.05
4	Male	Amesis, paclitaxel, Kytril	2.4 ± 0.09

presented in Table 3. The recoveries ranged from 101% to 105%. A statistical analysis using Student's *t*-test revealed that there were no significant differences between the expected and measured values, indicating the method's accuracy and reliability.

To assess the practicality and effectiveness of the proposed method for determining cisplatin, four 24 hour urine samples collected from patients taking cisplatin were analyzed according to standard addition method. The results of this analysis were presented in Table 4.

4 Conclusion

In this study, a nanoprobe composed of GQDs/PVA hydrogel nanocomposite was synthesized and used to detect cisplatin in urine samples. The results showed that the fluorescence emission of the nanocomposite was gradually enhanced by increasing the cisplatin concentration. A linear relationship was found between the fluorescence intensity and cisplatin concentration within the range of 4.3 to 25.0 ng mL^{-1}. The method's precision was high, with intra-day and inter-day variations of 1.8% and 3.6% respectively. Additionally, recoveries ranging from 101–105% in urine samples demonstrated the probe's potential for practical application in medical diagnosis. Overall, the GQDs/PVA hydrogel nanocomposite probe shows great promise for detecting cisplatin in medical settings.

Data availability

The datasets used and/or analysed during the current study are available from the corresponding author on reasonable request.

Conflicts of interest

The authors declare no conflict of interest.

Acknowledgements

This report is a part of the results of S. M. H. Pourmand's MSc thesis submitted to the Faculty of Pharmacy, Tabriz University of Medical Sciences, Tabriz, Iran, and supported by Tabriz University of Medical Science under grant number of 72850.

References

1 L. Galluzzi, L. Senovilla, I. Vitale, J. Michels, I. Martins, O. Kepp, M. Castedo and G. Kroemer, *Oncogene*, 2012, **31**, 1869–1883.
2 M. Kartalou and J. M. Essigmann, *Mutat. Res.*, 2001, **478**, 23–43.
3 P. J. Loehrer and L. H. Einhorn, *Annals of Internal Medicine: Clinical Cases*, 1984, **100**, 704–713.
4 S. R. McWhinney, R. M. Goldberg and H. L. McLeod, *Mol. Cancer Ther.*, 2009, **8**, 10–16.
5 M. Maillard, F. Le Louedec, F. Thomas and E. Chatelut, *Expert Opin. Drug Metab. Toxicol.*, 2020, **16**, 907–925.
6 L. Ye, M. Xiang, Y. Lu, Y. Gao and P. Pang, *Int. J. Electrochem. Sci.*, 2014, **9**, 1537–1546.
7 M. E. Bosch, A. R. Sánchez, F. S. Rojas and C. B. Ojeda, *J. Pharm. Biomed. Anal.*, 2008, **47**, 451–459.
8 M. Cui, L. Ding and Z. Mester, *Anal. Chem.*, 2003, **75**, 5847–5853.
9 S. J. Bannister, L. A. Sternson and A. J. Repta, *J. Chromatogr. A*, 1979, **173**, 333–342.
10 K. H. Kaushik, V. K. Sripuram, S. Bedada, N. Y. Reddy, G. I. Priyadarshini and K. R. Devarakonda, *Clin. Res. Regul. Aff.*, 2010, **27**, 1–6.
11 A. Zenker, M. S. Galanski, T. L. Bereuter, B. K. Keppler and W. Lindner, *J. Chromatogr. B*, 2000, **745**, 211–219.
12 K. Inagaki, S. Yonehara and Y. Kidani, *Chem. Pharm. Bull.*, 1985, **33**, 3369–3374.
13 R. Raghavan and J. A. Mulligan, *Drug Dev. Ind. Pharm.*, 2000, **26**, 423–428.
14 S. Nussbaumer, P. Bonnabry, J.-L. Veuthey and S. Fleury-Souverain, *Talanta*, 2011, **85**, 2265–2289.
15 S. Patel, R. Jamunkar, D. Sinha, T. K. Patle, T. Kant, K. Dewangan and K. Shrivas, *Trends Environ. Anal. Chem.*, 2021, **31**, e00136.
16 M. Bacon, S. J. Bradley and T. Nann, *Part. Part. Syst. Charact.*, 2014, **31**, 415–428.
17 G. Cao, *Nanostructures & Nanomaterials: Synthesis, Properties & Applications*, Imperial College Press, 2004.
18 X. Wang, J. Yu, W. Ji, M. Arabi, L. Fu, B. Li and L. Chen, *ACS Appl. Nano Mater.*, 2021, **4**, 6852–6860.
19 W. Ji, J. Yu, J. Cheng, L. Fu, Z. Zhang, B. Li, L. Chen and X. Wang, *ACS Appl. Nano Mater.*, 2022, **5**, 1656–1663.
20 U. S. Madduma-Bandarage and S. V. Madihally, *J. Appl. Polym. Sci.*, 2021, **138**, 50376.
21 F. Ullah, M. B. H. Othman, F. Javed, Z. Ahmad and H. M. Akil, *Mater. Sci. Eng., C*, 2015, **57**, 414–433.
22 C. Ruiz-Palomero, M. L. Soriano, S. Benitez-Martinez and M. Valcarcel, *Sens. Actuators, B*, 2017, **245**, 946–953.
23 F. Karchoubi and H. Pahlevani, *Journal of Applied Chemical Research*, 2019, **3**, 3–38.
24 M. Amjadi, J. L. Manzoori and T. Hallaj, *J. Lumin.*, 2014, **153**, 73–78.
25 P. Khanna, N. Singh, S. Charan, V. Subbarao, R. Gokhale and U. Mulik, *Mater. Chem. Phys.*, 2005, **93**, 117–121.

26 Z. Karimzadeh, A. Jouyban, A. Ostadi, A. Gharakhani and E. Rahimpour, *Anal. Chim. Acta*, 2022, **1227**, 340252.
27 M. Vandana, H. Devendrappa, P. D. Padova and G. Hegde, *Nanomaterials*, 2022, **12**, 3175.
28 Y.-N. Chen, L. Peng, T. Liu, Y. Wang, S. Shi and H. Wang, *ACS Appl. Mater. Interfaces*, 2016, **8**, 27199–27206.
29 D. Elumalai, B. Rodríguez, G. Kovtun, P. Hidalgo, B. Méndez, S. Kaleemulla, G. M. Joshi and M. T. Cuberes, *Nanomaterials*, 2023, **14**, 5.
30 S. Elfeky, *Journal of Environmental Analytical*, 2018, **5**, 1–5.
31 L. Li, A. Pandey and D. Werder, *J. Am. Chem. Soc.*, 2011, **133**, 1179.
32 Y. Chen and Z. Rosenzweig, *Anal. Chem.*, 2002, **74**, 5132–5138.
33 L. R. Cambrea, C. A. Yelton and H. A. Meylemans, in *Trace Materials in Air, Soil, and Water*, ACS Publications, 2015, pp. 195–210.
34 T.-W. Lin, N. Dhenadhayalan, H.-L. Lee, Y.-T. Lin, K.-C. Lin and A. Chang, *Sens. Actuators, B*, 2019, **281**, 659–669.
35 A. Hatefi, E. Rahimpour, M. Khoubnasabjafari, M. Edalat, V. Jouyban-Gharamaleki, S. Alvani-Alamdari, A. Nokhodchi, M. H. Pournaghi-Azar and A. Jouyban, *Microchim. Acta*, 2019, **186**, 1–8.
36 T. I. Chanu and D. P. Negi, *Chem. Phys. Lett.*, 2010, **491**, 75–79.
37 X. Sui, C. Luo, C. Wang, F. Zhang, J. Zhang and S. Guo, *Nanomedicine*, 2016, **12**, 1997–2006.
38 F. Nasrollahi, Y. R. Koh, P. Chen, J. Varshosaz, A. A. Khodadadi and S. Lim, *Mater. Sci. Eng., C*, 2019, **94**, 247–257.
39 Y. Ramos, C. Hernández, L. A. Fernandez, M. Bataller, E. Veliz and R. Small, *Quim. Nova*, 2011, **34**, 1450–1454.
40 S. Khumngern, J. Choosang, P. Kanatharana, P. Thavarungkul and A. Numnuam, *Talanta*, 2024, **267**, 125147.
41 H. Tafazoli, M. Safaei and M. R. Shishehbore, *Anal. Sci.*, 2020, **36**, 1217–1222.
42 K. Alhazzani, A. Z. Alanazi, A. M. Mostafa, J. Barker, M. M. El-Wekil and A.-M. B. H. Ali, *RSC Adv.*, 2024, **14**, 2380–2390.